Modelling of a Space-Based Ronchi Ruling Experiment for High-Precision Astrometry

S. SHAKLAN and S. PRAVDO
Jet Propulsion *Laborartory*
California *Institute of Technology*
4800 Oak Grove Dr.
Pasadena, CA 91109

G. GATEWOOD
Allegheny Observatory
Observatory Station
Pittsburgh, PA 15214

and

C. FTACLAS
Hughes Danbury Optical Systems, Inc.
100 Wooster Heights Rd.
Danbury, CT 06810

Abstract.

An end-to-end modelling program for an astrometric telescope employing a Ronchi ruling has been developed. The program models the aberrated images formed anywhere in the field-of-view. It then determines apparent centroids by simulating the motion of a Ronchi ruling across the field. Photo-electron statistics are included. A 6 term plate-constant model is used to determine the apparent motion of a target star within a reference frame as the object is re-observed through both ideal and perturbed optics. The modelling code is accurate at the sub-micro-arcsecond level.

Key words: Astrometry, planet detection, telescopes

1. Introduction

Ronchi rulings have been successfully employed in ground-based astrometric programs by several groups (Gatewood 1987, Buffington 1990). Stellar positions are measured by sliding the ruling across the image plane, repeatedly eclipsing the images of a target star and several reference stars. The number of lines between stars gives the approximate separation (in one dimension), while the phase difference between the periodic signals provides high precision.

On the ground, random differential motions caused by atmospheric turbulence have limited astrometric precision to about one milli-arcsecond. Improvements will come with larger telescopes located at superior sites. Shao and Colavita (1992) predict that with a 10 meter telescope located at Mauna Kea, one can achieve sub-100 microarcsecond precision.

Current technology for the manufacture of Ronchi rulings should allow at least an order of magnitude improvement beyond 100 microarcseconds. To realize microarcsecond precision, it will be necessary to launch an orbiting 1.5 m class telescope. A mission to do that called the Astrornetric Imaging Telescope (All') has been proposed, and is described elsewhere in these proceedings (Pravdo *et al.* 1993).

There are several important differences between ground- and space-based systems. On the ground, atmospheric turbulence can be counted on to smooth images

to a resolution well below the diffraction limit. Ground-based algorithms for determining the position of the star depend upon both image smoothness (no sidelobes) and random image motion (Gatewood 1987, Buffington 1990) . In space, images are diffraction limited and stable. The signal passed by the Ronchi ruling may have local minima due to diffraction rings, while aberrated images are not smoothed by atmospheric blurring.

The purpose of this paper is to describe the end-to-end modelling of a space-based astrometric telescope employing a Ronchi ruling as the metric. Our modelling codes function at the sub-microarcsecond level, and the algorithms are robust enough to allow for reasonable telescope perturbations. We begin this paper with the mathematical framework that describes the functionality of the ruling and noise characteristics of the detected signal. We then detail the implementation of a computer based end-to-end model as well as the plate constant model that is used to determine the astrometric precision of a field of stars. Finally, we present results of our modelling, including optical tolerancing of AIT and required integration times for several target stars.

2. Optical model

The principle components of a Ronchi ruling based astrometric system are the telescope, ruling, focal plane apertures, and detectors. The telescope, described below, should have low distortion, and a field-of-view sufficient for observing several reference stars surrounding the target star. The ruling is placed directly in the focal plane with no intervening optics. Behind the ruling are several movable apertures with fiber optics that carry starlight to the detectors. Each aperture collects the light from one star, and each photon-counting detector sees a periodic signal as the ruling is drawn across the field-of-view. Starlight is incident on the focal plane with a distribution given by $I(x, y)$. The Ronchi ruling is a periodic function given by $R(x - vt)$, where v is the velocity of the ruling and t is a relative time coordinate. The ruling is assumed to extend infinitely in the y direction, so that the power transmitted beyond the focal plane is given by the convolution of 1 with R:

$$P(t) = \int_{-\infty}^{\infty} \int_{-\infty}^{\infty} I(x, y) R(x - vt)\, dx\, dy \quad , \tag{1}$$

The power reaching the detector, P_d, is the component of P that passes through the focal plane aperture and is transmitted by the fibers.

The detected signal is given by

$$s(t) = \sum_{i=1}^{N} \delta(t - t_i) \quad , \tag{2}$$

where t_i is the arrival time of the ith photon. The probability of detecting a photoelectron at a given time follows Poisson statistics, with a mean rate determined by the instantaneous power $P_d(t)$.

The ruling serves as a spatial filter of the incident starlight. In the Fourier domain, one can see that all of the intrinsic information of the detected light is

localized to the first few Ronchi ruling harmonics. The Fourier transform of the detected signal is

$$\tilde{s}(f) = \sum_{i=1}^{N} \exp -2\pi j f t_i \,. \tag{3}$$

After averaging over positional and temporal statistics, the mean value is

$$\langle \tilde{s}(f) \rangle = \bar{N} \frac{\tilde{I}(f)\tilde{R}(f)}{\tilde{I}(0)\tilde{R}(0)} \quad , \tag{4}$$

where N is the total number of photons collected, I is now taken to be the line spread function $I(x) = \int I(x, y)\, dy$, and tilde over a symbol is used to indicate the Fourier transformed quantity. z is expressed as a temporal quantity via $t = x/v$.

Equation 4 demonstrates several important characteristics of detection with a Ronchi ruling. First, since the Fourier transform of a periodic function is a series of delta functions (the harmonics), all of the positional information must be derived from the harmonics. Since the true centroid is uniquely given by the slope of $\tilde{I}$ at f = O, the Ronchi ruling can not determine the true centroid unless it has an infinite period. (Thus, the harmonics sample $\tilde{I}$ infinitely close to the origin). Second, it is evident that a square-wave ruling is better than a sinusoidal ruling because the amplitude of R at the first harmonic is higher by $4/\pi$ for a square wave, and the square wave provides additional harmonics. Third, one can see that beyond the maximum spatial frequency passed by $\tilde{I}$, there is no information. Finally, higher harmonics are attenuated by $\tilde{I}$. The last two points demonstrate the importance of diffraction limited imaging, for aberrations reduce the amplitude of $\tilde{I}$.

It can be shown (Goodman and Belsher 1976) that the spectral density of the detected signal is given by

$$\langle |\tilde{s}(f)|^2 \rangle = \bar{N} + \left(\bar{N} \frac{\tilde{I}(f)\tilde{R}(f)}{\tilde{I}(0)\tilde{R}(0)} \right)^2 \quad , \tag{5}$$

so that one is left with the resulting white noise variance

$$\begin{aligned} \sigma_d^2 &= \langle |\tilde{s}(f)|^2 \rangle - | \langle \tilde{s}(f) \rangle |^2 \\ &= \bar{N} \quad . \end{aligned} \tag{6}$$

The characteristic white noise spectrum is used below in our centroid estimator.

Finally, we show that for a 50% duty cycle, the covariance of the harmonics is zero. It can be shown that the covariance of the noise is given by

$$\begin{aligned} \mathrm{Cov}(\Delta f) &\equiv \frac{1}{\sigma_d^2} (\langle \tilde{s}(f)\tilde{s}(f + \Delta f) \rangle - | \langle \tilde{s}(f) \rangle |^2) \\ &= \frac{\tilde{I}(\Delta f)\tilde{R}(\Delta f)}{\tilde{I}(0)\tilde{R}(0)} \quad . \end{aligned} \tag{7}$$

For a 50% duty cycle, only the odd harmonics exist. For a fundamental frequency of f_f, the A f between harmonics is $2f_f$. But $\tilde{R}(2f_f) =$ O, so that there is no

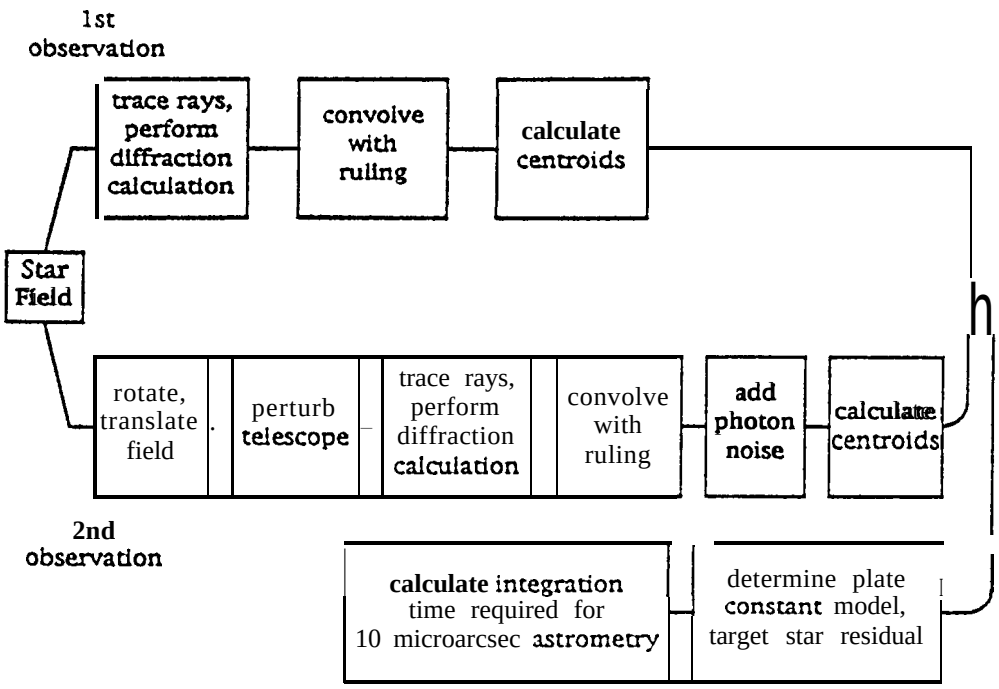

Fig. 1. Block diagram of end-to-end modelling process.

correlation. If, however, the duty cycle is changed, even harmonics appear. In that case, the correlation between adjacent harmonics is $\tilde{R}(f_f)$, which approaches $2/\pi$. Because of the large correlation between adjacent harmonics, there is little to be gained by using a duty cycle other than 50%.

3. End-to-end model

Our model consists of several star fields selected from a list of nearby stars, a ray trace/diffraction program, a model of the Ronchi ruling, a photon noise generator, and an astrometric analysis program. Figure 1 shows a schematic of the end-to-end modelling process. All software is executed on a Sun Spare 2 workstation.

3.1. IMAGING CODE

End-to-end modelling begins with a high-precision optical ray-trace and diffraction program called the Controlled Optics Modelling Package (COMP) (Redding and Breckinridge 1991).

COMP's ray-trace has been verified against the commercially available optical program CODE V (Optical Research Associates 1993). For AIT, we have shown

that COMP'S numerical precision is 20 nano-arcseconds for a bundle of 2600 rays traced through the system at field angles up to 10 arcminutes. The accuracy of the ray trace in terms of the centroid of the ray bundle is estimated by using larger and larger numbers of rays until the centroid no longer shifts. The interesting result of this study is that a small number of rays (e.g. 2000) gives accurate ***relative*** centroids at the sub-micro-arcsecond level, while the ***absolute*** centroids differ only by a multiplicative constant. In other words, by using a reasonably small number of rays, the system magnification is slightly off (by a fraction of a percent), but the quadratic and higher order distortion terms are accurately determined.

The diffraction calculation begins by tracing the rays backwards to the exit pupil of the system. A spherical phase term, with radius centered on the chief ray position in the image plane, is removed from the optical path of each ray. The remaining optical path defines the phase of the electric field at each grid point. The distribution is transformed by FFT to the image plane, where it is squared to yield the diffraction image. Typically, a 512 x 512 array is employed. Diffraction images are accurate even in the presence of large aberrations in off-axis images.

We find that diffraction centroids follow closely the ray centroids at the 30 μas level (after removal of a small linear magnification term). In theory, an image calculated by Fourier Transform of the exit pupil should have exactly the same centroid as the ray distribution (Lawrence *et al.* 1991). We believe that computational approximations account for this difference, which in any case is accommodated in the end-to-end model; the quadratic plate constant model described below accounts for this effect.

in Figure 2, we show how the chief ray, ray centroid, and diffraction centroid compare across AIT's 16 arcminute field-of-view

3.2. Ronchi ruling model

The Ronchi Ruling (RR) is modelled as a one-dimensional o]le-zero function whose period and length are both powers of 2. In this way, the harmonics are integers in the discrete frequency domain. A 50% duty cycle is used, but other duty cycles could easily be simulated.

As noted above, the true image centroid is given by the derivative of the image FT evaluated at the spatial frequency origin. For a shifted, but otherwise symmetric image, phase is directly proportional to spatial frequency. Any spatial frequency (i.e. any ruling harmonic) can be used to estimate the centroid. However, for asymmetric images, such as those containing coma, the centroid is still given by the phase slope at the origin, but the phase is no longer linear. (See, e.g., figs. 9 and 10 of Lawrence *et al.* 1991). Spatial frequency samples made away from the origin contain both centroid and asymmetry information. Since the RR is periodic, it passes only discrete spatial frequencies. There is no direct way (using a linear estimator) to determine the phase slope at the origin. Non-linear estimators, such as a matched filter, could be used, but they assume some *a priori* knowledge of the optical aberrations and arc sensitive to misalignments or deformation of the optics.

We have chosen to implement a simple linear estimator in which the phase slope is estimated as the weighted least-squares line passing through the first several

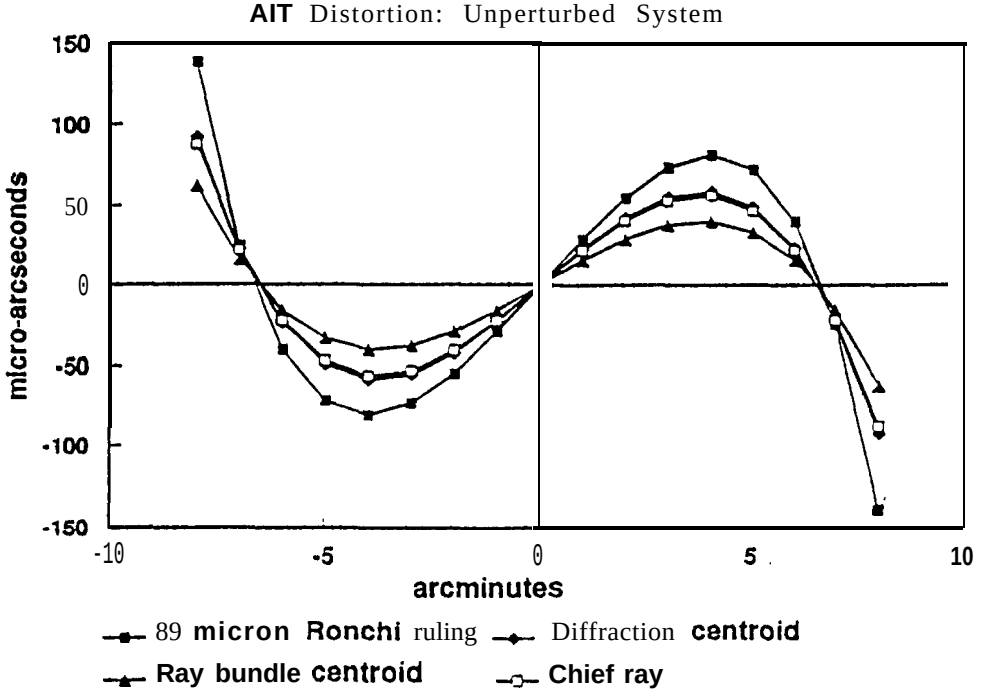

Fig. 2. Distortion in the Astrometric Imaging Telescope. A linear term (system magnification) has been removed.

ruling harmonics. Weighting is determined by the amplitude of the modulation. In practice, this is implemented by integrating the image in one dimension, computing its FFT, then multiplying by the FFT of the ruling. A least-squares routine is used to determine a line passing through the origin and the first several harmonics.

The noise of the centroid estimate can be derived from eqs. 6 and 7, where it is evident that the noise in the frequency domain is white and uncorrelated. At a given harmonic, the signal-to-noise ratio of the amplitude is given by

$$SNR_A = \sqrt{N}\frac{\tilde{I}(f)\tilde{R}(f)}{\tilde{I}(0)\tilde{R}(0)} \quad , \tag{8}$$

where N is the number of detected photoelectrons.

In the approximation $SNR >> 1$, the phase noise (in radians) is then given by

$$\sigma_p = 1/SNR_A \quad . \tag{9}$$

This approximation is always valid for integration times of several seconds or more on any of the 20 brightest stars in the field (as long as the ruling is neither too wide nor too narrow). The phase noise is used by the Ronchi ruling least squares routine to obtain a formal error on the phase slope. The phase slope and error are then converted to centroid position and centroid error σ_c. When a single harmonic

is used, the centroid error is

$$\sigma_c = \frac{\sigma_p}{2\pi} T \quad , \tag{10}$$

where T is the period of the ruling. For wide rulings, where higher harmonics are still well below the cutoff frequency of $\tilde{I}$, additional harmonics decrease σ_c by approximately $\sqrt{H}$, where H is the number of harmonics used. For narrow rulings, only the first harmonic makes a significant contribution.

As shown below, the optimum spacing in terms of the *SNR is* too sensitive to aberrations. Because of this sensitivity, we are forced to use a relatively wide ruling, increasing integration times above the theoretical limit.

3.3. ASTROMETRIC MODEL

AIT performs relative astrornetry, measuring the motion of a target star relative to a background frame. Over its lifetime, it will measure each target star several times per year. With each subsequent observation, the pointing, roll, focus, focal plane position, and optical components will change at some small level. The reference stars allow one to make an affine transformation between frames. We have found that a 3 term linear model is too sensitive to aberrations to be useful, Instead we use a 6 term quadratic model given hy

$$x' = a_0 + a_1 x + a_2 y + a_3 xy + a_4 x^2 + a_5 y^2 \tag{11}$$

where x and y are the coordinates of a star in the original frame, and x' is tile coordinate in subsequent, frames. y' is measured in separate observations. A least squares routine is used to perform the affine transformation. Each star is weighted according to its brightness and image quality. At least 6 reference stars are required for this model. Error propagation using this model has been discussed by Eichorn and Williams (1963).

The 6 term model is more light-efficient than a third order model that could account for the standard distortion term. We have found that the designed third order distortion (about ±100 micro-a arcseconds) is satisfactorily reduced by the quadratic model; target star errors are below 1 micro-arcsecond assuming that the telescope is repointed to within 10 arcseconds of the original frame.

4. Optical design

The ideal astrometric telescope has zero distortion and forms perfectly symmetric images across the field-of-view. No two-mirror design can achieve this, but a special class of Ritchey-Chretien designs can eliminate third order distortion, spherical aberration, and coma. The equations for determining this design have been given by Korsch (1990). The AIT design is driven by additional factors, such as the desire for a small secondary mirror to reduce sidelobes for another instrument, constrained overall length, and the need for a large collecting area (Pravdo *et al.* 1993). The current design has a 1.5 ni primary, ***44*** cm secondary, and a **22.6 m** effective **focal length.**

5. Telescope tolerances

As designed, AIT's ultimate astrometric limit is better than 10 micro-arcseconds. Motions of the secondary mirror, mirror contamination, mirror deformation, and background stars all affect the delicately balanced image symmetry and induce astrometric errors,

To test our sensitivity to these perturbations, we generate two observations: a first observation, with the target star centered in the field, and all optics operating perfectly; and a second observation where a part or parts of the system are perturbed. In the second observation, we assume a pointing error of 2 arcseconds and roll error of 1°. The system is perturbed by modifying the COMP telescope prescription before tracing rays.

Figure 3 shows the field distortion when the secondary is recentered by 100 microns perpendicular to the telescope axis. The true ceutroids are well behaved, despite significant aberrations. The Ronchi ruling "centroid," however, now has 2 milli-arcseconds of error. This is due to the non-symmetric interaction of the field-independent coma with design astigmatism. A 100 micron decenter causes less that 0.01 waves r.m.s. of aberration, an indication of the sensitivity of the ruling to misalignments. To achieve 10 micro-arcsecond precision (assuming no in-flight calibration), decentcr of the secondary must be maintained to 10 microns, while tilt must be maintained to 7 arcseconds.

Fortunately, astrometric precision is highly insensitive to "breathing" of the metering truss. When the truss expands, the primary-secondary spacing changes, but image symmetry is not affected. The plate-scale model accounts for the focal plane scale change. Secondary motions of up to $\pm$ 0.5 mm are permitted.

We have also found that the end-to-end model is rather insensitive to the conic constants of both the primary and secondary mirrors. For this simulation, the conies are assumed to have an error in both the initial and final observations. We find that the conies can be in error by more than Δk >0.01 on both mirrors.

The Ronchi ruling used for these simulations has a period of 89 μm corresponding to 0.8 arcseconds in the focal plane. This is 7 times larger than the optimal (for integration time) ruling, increasing integration time by a factor of 7.

To improve tolerancing requirements, in-flight calibration can yield information on focal-plane distortion. The general idea of the scheme is to observe a set of three or more bright stars separated by $\approx$ 1 arcminute at several points in the field. The apparent star separations are used to estimate the field dependence of the distortion. Tolerance requirements are relaxed by a factor of $\approx$ 5.

6. Integration times for several target stars

A set of 10 sample fields was chosen from a list of nearby stars. The set represents a wide range of magnitudes of both target and reference stars. The brightest 25 stars within an 8 arcminute radius of the target star arc used to define the reference frame. We used the first 3 harmonics to estimate the centroid of each star. The Table gives the integration time required to reduce the target star positional error to 10 micro-arcseconds. Columns 3 and 4 indicate the average number of detected

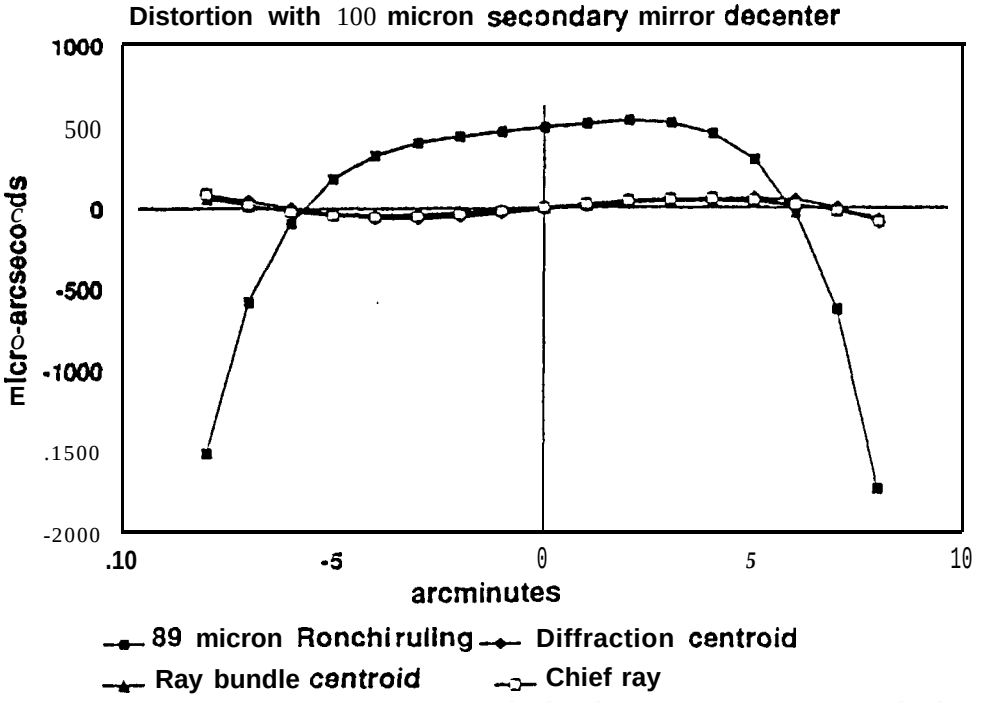

Fig. 3. Distortion when the secondary mirror is displaced by 100 microns perpendicular to the optical axis. Chief ray, ray centroid, and diffraction distortion remain well behaved. The Ronchi ruling, however, is sensitive to the field-independent coma of the recentered system.

photons for the target star and reference frame, respectively. These numbers are based upon instrumental throughput of 2% which includes optical losses in the telescope, ruling and fiber optics, and the quantum efficiency of the detectors.

The target stars are divided into two groups. In the upper group, the target star is fainter than the reference frame. In the second group, the reference frame limits integration time. One can draw the general conclusion that brighter reference frames are better, but that is not always the case. For example, SAO 082706 requires a significantly longer integration than SAO 062377. The discrepancy is due to the light distribution in the reference frame.

7. Conclusion

The model described herein demonstrates that a Ronchi ruling space-based experiment such as AIT can achieve astrometric measurement accuracy of 10 micro-arcseconds. Most importantly, this is not an idealized model. Even in the presence of pointing errors and optical aberrations,, the experimental design is sufficiently robust to perform at the design accuracy.

TABLE I
Integration times for 10 micro-arcsecond astrometry

Star	m_v	Targ. Phot/s x 10^3	Ref. Phot/s x 10^3	Req'd T(s)
Ross 128	11.10	48	3534	7992
SAO 122963	9.54	210	3592	1303
SAO 065525	8.10	764	1326	812
SAO 082706	4.26	25309	786	5184
SAO 062377	7.49	1328	495	3387
SAO 157844	4.74	17509	1687	2143
SAO 080104	5.14	12114	1788	918
SAO 177866	4.93	14564	1515	756
SAO 062738	6.45	3336	1637	645
SAO 200163	4.62	19199	3338	317

Acknowledgements

We **would like to acknowledge many useful conversations with** H. Kadogawa, E. Levy, R. Terrile, A. Buffington, A. Nonnenmacher, K. Shu, and B. Levine. This work was carried out at the Jet Propulsion Laboratory, California Institute of Technology, under contract with the National Aeronautics and Space Administration,

References

Buffington, A., and **Geller,** M. A.: 1990, 'Photoelectric **Astrometric** Telescope Using **a Ronchi** Ruling', ***P. A.S.P.*** 102, 200.

Eichorn, E., **and Williams, C. A.: 1963, 'On the systematic accuracy of photographic astrometric data',** ***Ap. J.*** **68, 221.**

Gatewood, G. D.: 1987 'The multichannel **astrometric** photometer and atmospheric limitations **in the measurement of relative positions',** ***A .J.*** **94, 213.**

Goodman, J.W. and **Belsher** J. F.: 1976, 'Photon limited images and their restoration," Rome **Air Development Center Technical Report** RADC-TR-76-50.

Korsch, D.: **1990, in** ***Astrometric Telescope*** **Facility** ***(ATF) FY'89*** Final ***Report,*** JPL pub. D-7113, 23.

Lawrence, G. N., Huang, C., Levy, E. H., McMillan, R. S.: 1991, 'High accuracy image centroiding with a moving Ronchi ruling', ***Opt.*** **Engineer. 30, 598.**

Optical Research Associates, 1993: CODE V is a proprietary product of Optical Research Associates, 550 N. Rosemead Blvd., Pasadena CA 91107.

Pravdo, S. ***et a/.*****, 1993: 'The Astrometric Imaging Telescope: detection of planetary systems with imaging and astrometry', (This volume).**

Redding, D. **and Breckinridge, W.: 1991, 'Optical Modeling for Dynamics and Control Analysis',** ***J. G.C.D*** **14, 1021.**

Shao, M. **and Colavita, M. M.: 1992 'Potential of long-baseline infrared interferometry for narrow-angle astrometry,'** ***Astron. Astrophys.*** **262, 353.**